

Matrix Isolation | *Very Important Paper*
VIP **Generation and Identification of the Linear OCBNO and OBNC O Molecules with 24 Valence Electrons**

 Guohai Deng^{+, [a]}, Sudip Pan^{+, [b, c]}, Jiaye Jin,^[a] Guanjun Wang,^[a] Lili Zhao,^[b] Mingfei Zhou,^{*, [a]} and Gernot Frenking^{*, [b, c]}

Abstract: Two structural isomers containing five second-row element atoms with 24 valence electrons were generated and identified by matrix-isolation IR spectroscopy and quantum chemical calculations. The OCBNO complex, which is produced by the reaction of boron atoms with mixtures of carbon monoxide and nitric oxide in solid neon, rearranges to the more stable OBNC O isomer on UV excitation. Bonding

analysis indicates that the OCBNO complex is best described by the bonding interactions between a triplet-state boron cation with an electron configuration of $(2s)^0(2p_\sigma)^0(2p_\pi)^2$ and the CO/NO⁻ ligands in the triplet state forming two degenerate electron-sharing π bonds and two ligand-to-boron dative σ bonds.

Introduction

The structure and bonding of main group compounds have been the focus of extensive theoretical and experimental investigations.^[1] Many species containing five second-row element atoms with 24 valence electrons are experimentally known,^[2–17] some of which have been included in common inorganic chemistry textbooks.^[2] The structure and bonding of the symmetric EL₂ isomers (E = B⁻, C, N⁺; L = CO, N₂, NO, etc.) have received particular attention.^[3–6] The carbon suboxide C₃O₂ is linear in the solid state, and is conventionally described as a linear cumulene O=C=C=O.^[7] However, high-resolution spectroscopic and theoretical investigations indicated that the gas-phase molecule is bent with an angle of 156° at the cen-

tral carbon atom.^[8] The bent structure of carbon suboxide can be well interpreted in terms of donor–acceptor bonding between two carbonyl ligands and a neutral carbon atom in its ¹D excited state with an electron configuration of $(2s)^0(2p_\sigma)^2(2p_\pi)^0$.^[6, 28]

The donor–acceptor bonding model straightforwardly explains the different geometric structures of the isoelectronic EL₂ series with E = N⁺, C, and B⁻.^[29] The dicyanamide anion [N(CN)₂]⁻, firstly synthesized in 1925,^[9] is a stable pseudohalogen ion with a bent structure.^[10] The N⁺(NN)₂ and N⁺(CO)₂ ions have also been synthesized as bulk salts,^[11, 12] and both were calculated and crystallographically determined to have strongly bent equilibrium geometries as well. The larger bending angle of carbon suboxide relative to the N⁺L₂ (L = N₂, CO, CN⁻) complexes comes from the stronger OC←C→CO π -backdonation interaction compared with that in the N⁺L₂ complexes.^[28] The negatively charged B(CO)₂⁻ complex was generated in solid noble-gas matrices.^[13] It was characterized to have a linear structure that is best described in terms of donor–acceptor interactions between a boron atom with a valence electron configuration of $(2s)^0(2p_\sigma)^0(2p_\pi)^4$ and CO ligands with very strong OC←B→CO π backdonation. Herein, we report the generation and spectroscopic characterization of two additional five-atom, 24-valence-electron molecules, OCBNO and OBNC O, in solid neon. A detailed bonding analysis indicates that the linear OCBNO species is best described by the bonding between a triplet-state boron cation with an electron configuration of $(2s)^0(2p_\sigma)^0(2p_\pi)^2$ and the CO/NO⁻ ligands in the electronic triplet state forming two electron-sharing π bonds and two ligand-to-boron dative σ bonds.

[a] G. Deng,⁺ Dr. J. Jin, Prof. Dr. G. Wang, Prof. Dr. M. Zhou
 Collaborative Innovation Center of Chemistry for Energy Materials
 Department of Chemistry, Shanghai Key Laboratory of
 Molecular Catalysts and Innovative Materials, Fudan University
 Shanghai 200438 (P.R. China)
 E-mail: mfzhou@fudan.edu.cn

[b] Dr. S. Pan,⁺ Prof. L. Zhao, Prof. G. Frenking
 Institute of Advanced Synthesis, School of Chemistry and
 Molecular Engineering, Nanjing Tech University, Nanjing 211816 (P.R. China)
 E-mail: frenking@chemie.uni-marburg.de

[c] Dr. S. Pan,⁺ Prof. G. Frenking
 Fachbereich Chemie, Philipps-Universität Marburg
 Hans-Meerwein-Strasse 4, 35043 Marburg (Germany)

[*] These authors contributed equally to this work.

 Supporting information and the ORCID identification number(s) for the author(s) of this article can be found under:
<https://doi.org/10.1002/chem.202003886>.

 © 2020 The Authors. Chemistry - A European Journal published by Wiley-VCH GmbH. This is an open access article under the terms of the Creative Commons Attribution Non-Commercial NoDerivs License, which permits use and distribution in any medium, provided the original work is properly cited, the use is non-commercial and no modifications or adaptations are made.

Results and Discussion

Experimental results

The title species were prepared by the reaction of laser-ablated boron atoms with mixtures of carbon monoxide and nitric oxide in solid neon, and were detected by IR absorption spectroscopy with isotopic substitutions.^[18] The IR spectra in the 2360–1960 and 1500–1440 cm^{-1} regions obtained by using a ^{10}B -enriched target and a 0.05% $\text{CO} + 0.05\%$ $^{15}\text{NO}/\text{Ne}$ mixture with relatively low ablation laser energy (≈ 5 mJ/pulse) are shown in Figure 1. After sample deposition, strong absorption bands due to ^{10}BCO ($2014.2/2012.0$ cm^{-1}) and $^{10}\text{B}(\text{CO})_2$ (2031.1 cm^{-1}) are observed,^[13,19] which increase on annealing but decrease on UV/Vis irradiation. Species involving more than one boron atom, such as BBCO ,^[20] OCBBCO ,^[21] and BBNN ,^[22] which were reported previously to be the major products from the reactions of laser-ablated boron atoms with CO or N_2 , are barely observed. However, the BBCO (2043.6 cm^{-1}) and OCBBCO (2033.1 cm^{-1}) absorptions are clearly observed to increase on annealing with relatively high ablation laser energy. A group of absorptions (labeled **A** in Figure 1) appear on annealing to 10 K, and increase together on annealing to 12 K, but are completely destroyed on UV irradiation with a high-pressure mercury arc lamp. With the disappearance of group **A** absorption bands, a group of new absorption bands (labeled **B**) are produced. Similar experiments were performed with other isotopically labeled compounds including ^{15}NO , ^{13}CO , and C^{18}O , as well as a natural-abundance boron target. The spectra in selected regions for different isotopically labeled

samples and mixtures are shown in Figures S1–S5 of the Supporting Information. The band positions are listed in Table 1.

Species **A** is assigned to the OCBNO complex. The spectra for different isotopically labeled samples (Figures S2 and S3 of the Supporting Information) confirm that this species involves one boron atom, one CO ligand, and one NO ligand. Four bands at 2148.5, 2111.4, 1999.3, and 1472.5 cm^{-1} are observed for $\text{OC}^{10}\text{B}^{15}\text{NO}$ (Figure 1). However, only two or three bands are observed for the other isotopomers (Figure S1 of the Supporting Information and Table 1). The 2117.0 cm^{-1} band in the $^{10}\text{B} + \text{CO} + \text{NO}/\text{Ne}$ experiment shows quite large boron, carbon, and oxygen isotopic shifts (Table 1) and can be assigned to the BCO stretching mode (ν_1) of OC^{10}BNO . The 1999.3 cm^{-1} band of $\text{OC}^{10}\text{B}^{15}\text{NO}$ should be assigned to the BNO stretching mode (ν_2). This mode is not observed experimentally for the other isotopomers, due to weakness or overlap with the strong BCO or $\text{B}(\text{CO})_2$ absorption bands. The lowest band (1478.8 cm^{-1} for OC^{10}BNO) shows quite a large boron isotopic shift and is attributed to the OC-B-NO stretching mode (ν_3). The highest band at 2155.5 cm^{-1} for OC^{10}BNO cannot be assigned to a fundamental mode and is attributed to a combination mode ($\nu_3 + \nu_4$). It gains IR intensity through Fermi resonance with the ν_1 mode. This combination mode for the $\text{O}^{13}\text{C}^{10}\text{BNO}$ isotopomer is missing due to the disappearance of Fermi resonance.

Species **B** with two absorptions at 2331.1 and 2113.4 cm^{-1} is assigned to O^{10}BNCO , a structural isomer of OC^{10}BNO . The 2331.1 cm^{-1} band shows very small ^{11}B isotopic shift but quite large ^{15}N , ^{13}C , and C^{18}O isotopic shifts (Table 1). The band position and isotopic shifts indicate that it is an NCO stretching vibration.^[23] The experiments with isotopically labeled mixtures

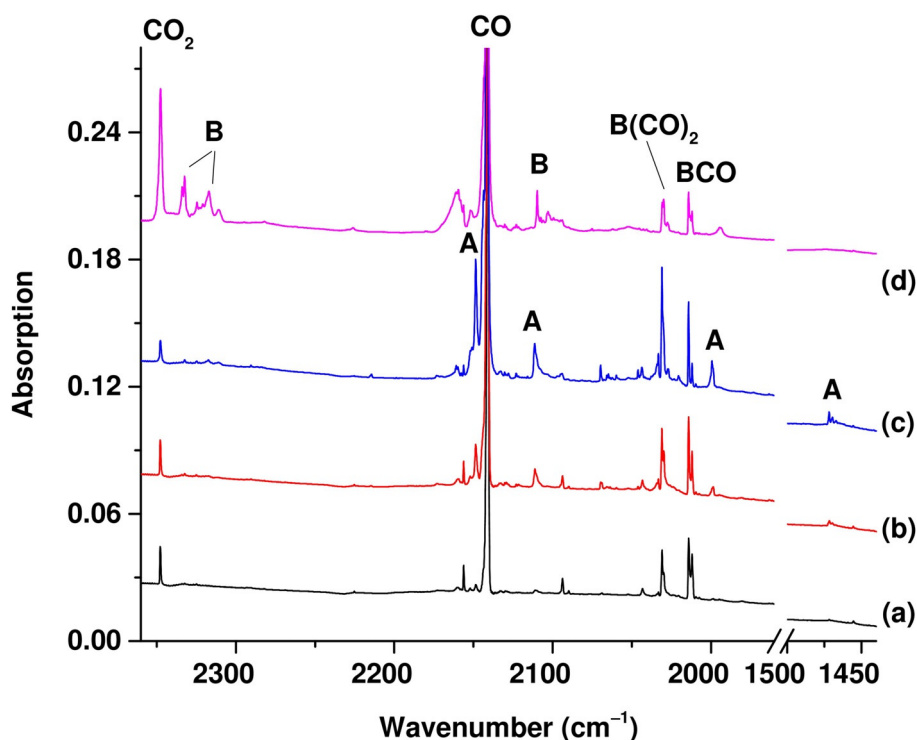


Figure 1. IR spectra in the 2360–1960 and 1500–1440 cm^{-1} regions from codeposition of laser-ablated boron (^{10}B -enriched) atoms with 0.05% $\text{CO} + 0.05\%$ ^{15}NO in neon. a) After 30 min of sample deposition at 4 K. b) After annealing to 10 K. c) After annealing to 12 K. d) After 15 min of UV/Vis ($250 < \lambda < 580$ nm) irradiation. **A:** $\text{OC}^{10}\text{B}^{15}\text{NO}$; **B:** $\text{O}^{10}\text{B}^{15}\text{NCO}$.

Table 1. Observed (in Ne) and computed (CCSD(T)-Full/aug-cc-pVTZ level of theory) vibrational frequencies [cm^{-1}] of OCBNO (**A**) and OBNCO (**B**). The calculated numbers in italics refer to vibrational modes that have not been observed experimentally.

	^{10}B					^{11}B				
	CO/NO	CO/ ^{15}N O	$\Delta^{[a]}$	^{13}C O/NO	$\Delta^{[a]}$	C^{18}O /NO	$\Delta^{[a]}$	CO/NO	$\Delta^{[a]}$	
OCBNO (A)	2155.5	2148.5	−7.0	— ^[b]		2134.2	−21.3	2131.5	−24.0	$\nu_3 + \nu_4$
	2117.0 — ^[b]	2111.4 1999.3	−5.6	2090.4 — ^[b]	−26.6	2097.1 — ^[b]	−19.9	2091.3 — ^[b]	−25.7	ν_1
	1478.8	1472.5	−6.3	1478.3	−0.5	1469.4	−9.4	1448.8	−30.0	ν_3
OBNCO (B)	2331.1	2317.9	−13.2	2272.9	−58.2	2311.0	−20.1	2329.7	−1.4	ν_1
	2113.4	2109.8	−3.6	2111.6	−1.8	2110.9	−2.5	2046.7	−66.7	ν_2
	Calculated									
OCBNO (A)	2171.2 (2144.1) ^[c]	2161.3 (2132.3) ^[c]	−9.9	2167.0 (2148.3) ^[c]	−4.2	2148.1 (2130.1) ^[c]	−23.1	2140.9 (2118.6) ^[c]	−30.3	$\nu_3 + \nu_4$
	2193.1 (2122.0) ^[c]	2185.2 (2116.7) ^[c]	−7.9	2165.1 (2106.5) ^[c]	−28.0	2180.0 (2147.0) ^[c]	−13.1	2166.5 (2103.9) ^[c]	−26.6	ν_1
	1979 ^[d]	1917 ^[d]		1804 ^[d]		1901 ^[d]		1956 ^[d]		
	2087.1 (2036.0) ^[c] [1] ^[d]	2058.0 (2008.6) ^[c] [20] ^[d]	−29.1	2060.6 (2025.0) ^[c] [106] ^[d]	−26.5	2065.7 (2027.9) ^[c] [31] ^[d]	−21.4	2071.0 (2030.2) ^[c] [43] ^[d]	−16.1	ν_2
OBNCO (B)	1513.6 (1481.8) ^[c] [165] ^[d]	1506.1 (1476.8) ^[c] [174] ^[d]	−7.5	1513.3 (1490.8) ^[c] [169] ^[d]	−0.3	1504.0 (1481.4) ^[c] [178] ^[d]	−9.6	1482.7 (1460.3) ^[c] [119] ^[d]	−30.9	ν_3
	2452.5 (2386.0) ^[c] [1885] ^[d]	2434.3 (2371.3) ^[c] [1807] ^[d]	−18.2	2391.1 (2319.7) ^[c] [1907] ^[d]	−61.4	2439.0 (2376.4) ^[c] [1896] ^[d]	−13.5	2451.3 (2394.0) ^[c] [1820] ^[d]	−1.2	ν_1
	2163.5 (2115.6) ^[c] [425] ^[d]	2160.0 (2116.8) ^[c] [466] ^[d]	−3.5	2159.4 (2114.2) ^[c] [332] ^[d]	−4.1	2160.4 (2120.2) ^[c] [393] ^[d]	−3.1	2094.0 (2055.3) ^[c] [436] ^[d]	−69.5	ν_2
	[a] Frequency shift relative to ^{10}B /CO/NO. [b] Not observed due to weakness or overlap with other absorption bands. [c] Anharmonic correction obtained at the B2PLYP/aug-cc-pVTZ level of theory added with the CCSD(T) frequencies. [d] The values in brackets are the intensities at the B2PLYP/aug-cc-pVTZ level of theory.									

(Figure S4 of the Supporting Information) confirm that the 2331.1 cm^{-1} mode only involves one NCO subunit. The 2113.4 cm^{-1} band exhibits quite a large ^{11}B isotope shift (66.7 cm^{-1}) but very small ^{15}N , ^{13}C , and C^{18}O isotopic shifts. The band position and isotopic shift imply that it is a terminal B–O stretching vibration and involves only one BO subunit.^[24] The very small oxygen isotopic shift for the C^{18}O sample implies that the oxygen atom of the terminal BO subunit comes from the NO reactant rather than CO.

Theoretical results

To validate the experimental assignment and to gain deep insight into the equilibrium geometries, electronic structures, and chemical bonding of the experimentally observed OCBNO (**A**) and OBNCO (**B**) isomers, quantum chemical calculations were performed (see Supporting Information for details). Geometric optimizations were performed on various possible structures in the electronic singlet and triplet states for different isomers of BCNO_2 at the CCSD(T)-Full/cc-pVTZ level of theory. The observed species were further reoptimized at the CCSD(T)-Full/aug-cc-pVTZ level of theory. Unless otherwise stated, all theoretical data in this work were calculated at this level of theory. Figure 2 shows the geometries of OCBNO (**A**) and OBNCO (**B**) and two other isomers **C** and **D**, which were not observed in our experiment. The geometries of 11 further isomers, which are more than $130 \text{ kcal mol}^{-1}$ higher in energy than the global energy minimum **B**, are shown in Figure S6 of the Supporting Information.

The OBNCO (**B**) molecule is predicted to have an electronic singlet ground state with linear structure, which is the global energy-minimum form of the BCNO_2 species. The OCBNO (**A**) isomer also has a singlet ground state with a linear structure. It lies $111.9 \text{ kcal mol}^{-1}$ higher than the global energy-minimum structure **B**. The calculated B–N distance in **A** (1.270 \AA) is significantly shorter than the B–C bond (1.408 \AA). The calculated B–N bond length is about the same as the sum of the covalent radii of triple-bonded boron and nitrogen atoms reported by Pyykko and co-workers (1.27 \AA).^[25] The B–C bond is longer than a typical $\text{B}=\text{C}$ bond (1.33 \AA)^[25] but is slightly shorter than a $\text{B}=\text{C}$ bond (1.45 \AA).^[26] The isomers **C** and **D** are lower in energy than **A** but were not observed in our experiments. Structure **C** also has an electronic singlet state and exhibits a rare bonding situation in which a significantly stretched O_2 molecule is bonded side-on to the terminal boron atom of a linear NCB moiety. Isomer **D** is the energetically lowest lying species in the electronic triplet state. The nonlinear structure features a BO fragment in which the boron atom is bonded to a nearly linear OCN species.

The calculated vibrational frequencies and isotopic frequency shifts of **A** and **B** are listed in Table 1. The agreement between the calculated frequencies and the experimental values is quite good. This holds even for the absolute values of the theoretical data when the harmonic frequencies at the CCSD(T)-Full/aug-cc-pVTZ level of theory are corrected by anharmonic contributions calculated at the B2PLYP/aug-cc-pVTZ level of theory. The only discrepancy between theory and experiment appears for the combination mode ($\nu_3 + \nu_4$), which is

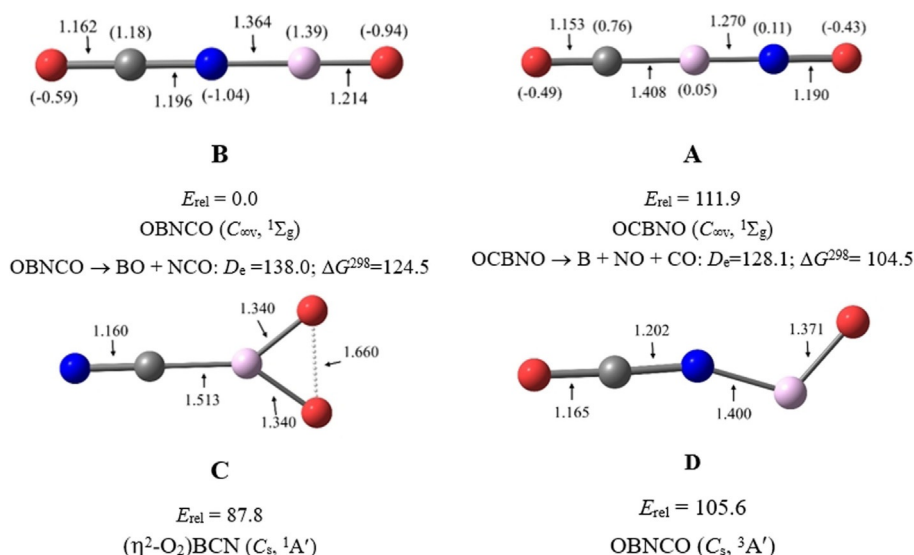


Figure 2. Geometries of the four energetically lowest lying BNCO₂ isomers A–D calculated at the CCSD(T)-Full/aug-cc-pVTZ level of theory for A and B and at the CCSD(T)-Full/-cc-pVTZ level of theory for C and D. Bond lengths are given in Å. The natural partial charges are given in parentheses. The relative energies and bond dissociation energies D_e at 0 and 298 K are in kcal mol⁻¹.

calculated to be slightly below the fundamental mode ν_1 . Since IR intensities at the CCSD(T)-Full/aug-cc-pVTZ level of theory are not available, the IR intensities calculated at the B2PLYP/aug-cc-pVTZ level of theory are listed. The complete set of calculated frequencies and intensities of all BCNO₂ isomers is given in the Supporting Information (Table S1).

The electronic structures of OCBNO (A) and OBNCO (B) were analyzed in order to understand the bonding situation in both species. The calculated natural partial charges shown in Figure 2 suggest that OBNCO can be described as bonding between a boronyl cation (BO^+) and an isocyanate NCO^- anion. The boronyl cation fragment has a very short bond length of 1.214 Å, indicating a robust $\text{B}\equiv\text{O}$ bond.^[27]

The bonding of linear OCBNO (A) is of particular interest. It has been shown that the symmetric isoelectronic EL_2 species ($\text{E}=\text{B}^-, \text{C}, \text{N}^+, \text{L}=\text{CO}, \text{N}_2$ etc.) are well described by a donor-acceptor bonding model involving not only $\text{L}\rightarrow\text{E}\leftarrow\text{L}$ σ -donation, but also strong $\text{L}\leftarrow\text{E}\rightarrow\text{L}$ π backdonation.^[3–6, 28, 29] The cen-

tral boron anion in the linear $\text{B}(\text{CO})_2^-$ anion has an $(2s)^0(2p_\sigma)^0(2p_\pi)^4$ electron configuration in which B^- leads to strong $\text{OC}\leftarrow\text{B}^-\rightarrow\text{CO}$ π backdonation.^[13] In contrast, the C_3O_2 , $\text{N}^+(\text{CO})_2$, and $\text{N}^+(\text{NN})_2$ species all have nonlinear structures due to weaker $\text{L}\leftarrow\text{E}\rightarrow\text{L}$ π backdonation with the central atoms in their excited ${}^1\text{D}$ state with electron configuration of $(2s)^0(2p_\sigma)^2(2p_{\pi\perp})^2(2p_{\pi\parallel})^0$. Figure 3 shows the HOMOs of OCBNO in the singlet ground state, which provide a first insight into the chemical bonds. The doubly degenerate HOMOs are B–C and B–N bonding π orbitals, which comprise B 2p AOs and antibonding π^* MOs of CO and NO ligands. The doubly degenerate HOMO–1 and HOMO–2 are primarily C–O and N–O π -bonding orbitals. HOMO–3 and HOMO–4 are BCO and BNO σ -bonding orbitals, respectively.

We calculated the interaction between the central boron atom and the $[\text{OC}\cdots\text{NO}]$ ligands with the EDA-NOCV method^[30] using several charges and electron configurations for the interacting moieties. In this way, it is possible to identify the best

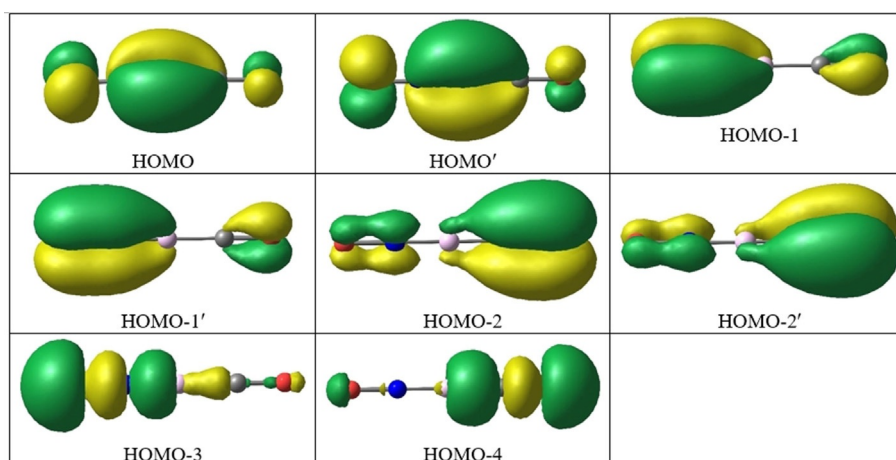


Figure 3. Shape of the energetically highest-lying occupied molecular orbitals of the singlet ground state OCBNO molecule A.

description of the bonding situation in a molecule. It has been shown in numerous studies that the smallest change in the associated orbital interaction ΔE_{orb} is a faithful account of the type of bonding. This has been demonstrated for a variety of chemical bonds.^[31] Table S2 shows that the lowest value for ΔE_{orb} is found when the interacting fragments in OCBNO (**A**) are B^+ in the electronic triplet state ^3D with the electron configuration $(2s)^0(2p_{\sigma})^0(2p_{\pi})^1(2p_{\pi})^1$ and $[\text{OC}\cdots\text{NO}]^-$ also in the triplet state with two unpaired electrons in the orthogonal π orbitals. Table 2 gives a full account of the numerical results, which show the strength of the different orbital interactions.

Table 2. EDA-NOCV results of OCBNO molecule A at the M06-2X/TZ2P//CCSD(T)-Full/aug-cc-pVTZ level taking $[\text{B}]^+$ (^3T , $(2s)^0(2p_{\sigma})^0(2p_{\pi})^1(2p_{\pi})^1$) + $[\text{OC}\cdots\text{NO}]^-$ (^3T) as interacting fragments. Energies are in kcal mol ⁻¹ .		
Energies	Orbital interaction	$[\text{B}]^+$ (^3T , $(2s)^0(2p_{\sigma})^0(2p_{\pi})^1(2p_{\pi})^1$) + $[\text{OC}\cdots\text{NO}]^-$ (^3T)
ΔE_{int}		-585.6
ΔE_{Pauli}		99.8
$\Delta E_{\text{Metahybrid}}$		25.7
$\Delta E_{\text{elstat}}^{[a]}$		-244.6 (34.4%)
$\Delta E_{\text{orb}}^{[a]}$		-466.5 (65.6%)
$\Delta E_{\text{orb}(1)}^{[b]}$	$[\text{B}]^+ - [\text{OC}\cdots\text{NO}]^-$ electron-sharing π bond	-103.3 (22.1%)
$\Delta E_{\text{orb}(2)}^{[b]}$	$[\text{B}]^+ - [\text{OC}\cdots\text{NO}]^-$ electron-sharing π bond	-103.3 (22.1%)
$\Delta E_{\text{orb}(3)}^{[b]}$	$[\text{B}]^+ \leftarrow [\text{OC}\cdots\text{NO}]^-$ (+, -) σ donation	-141.3 (30.3%)
$\Delta E_{\text{orb}(4)}^{[b]}$	$[\text{B}]^+ \leftarrow [\text{OC}\cdots\text{NO}]^-$ (+, +) σ donation	-78.8 (16.9%)
$\Delta E_{\text{rest}}^{[b]}$		-39.8 (8.6%)

[a] The values in parentheses give the percentage contribution to the total attractive interactions $\Delta E_{\text{elstat}} + \Delta E_{\text{orb}}$. [b] The values in parentheses give the percentage contribution to the total orbital interactions ΔE_{orb} .

There are two rather strong degenerate electron-sharing π interactions between B^+ and $[\text{OC}\cdots\text{NO}]^-$ of 103.3 kcal mol⁻¹ each and one stronger (-141.3 kcal mol⁻¹) and one weaker (-78.8 kcal mol⁻¹) dative bonds $\text{OC} \rightarrow \text{B} \leftarrow \text{NO}$, which provide 92% of the total interaction ΔE_{orb} . The remaining orbital interactions come from polarization of the ligand orbitals. Figure 4 shows the associated deformation densities $\Delta\rho_{(1)-(4)}$ of the four orbital terms. The π interactions go along with charge migration from boron to the ligands (red \rightarrow blue), whereas the σ donation shows as expected the opposite charge migration from the ligands to boron. Note that the magnitude of the charge migration, which is given by the eigenvalues $|\nu_n|$, is much larger for σ donation than for π backdonation. The magnitude of the charge migration does not correlate with the strength of the interactions.

A closer look at the deformation densities of the degenerate π interactions $\Delta\rho_{(1)}$ and $\Delta\rho_{(2)}$ shows that there is also a red area of charge depletion at the nitrogen atoms, which together with the red area at boron and the blue area of charge concentration between boron and nitrogen atoms signals the formation of B-N π bonding. In contrast, the B-C π region shows only some charge donation $\text{B} \rightarrow \text{CO}$. We analyzed the bonding situation in OCBNO (**A**) also with the Adaptive Natural Density Partitioning (AdNDP) method developed by Boldyrev and Zubarev,^[40] which is particularly suited for multicenter bonds. Figure 5 shows the 5c-2e π orbitals of **A**. Clearly, the π bonding is mainly in the B-N region with little π bonding between boron and carbon. This agrees with the results of the NBO analysis, which suggests that the best Lewis structure for **A** has a triple bond between boron and nitrogen atoms but only a single bond between boron and carbon atoms.

The spectra shown in Figure 1 clearly show that the OCBNO molecule is formed by the reactions of ground-state boron

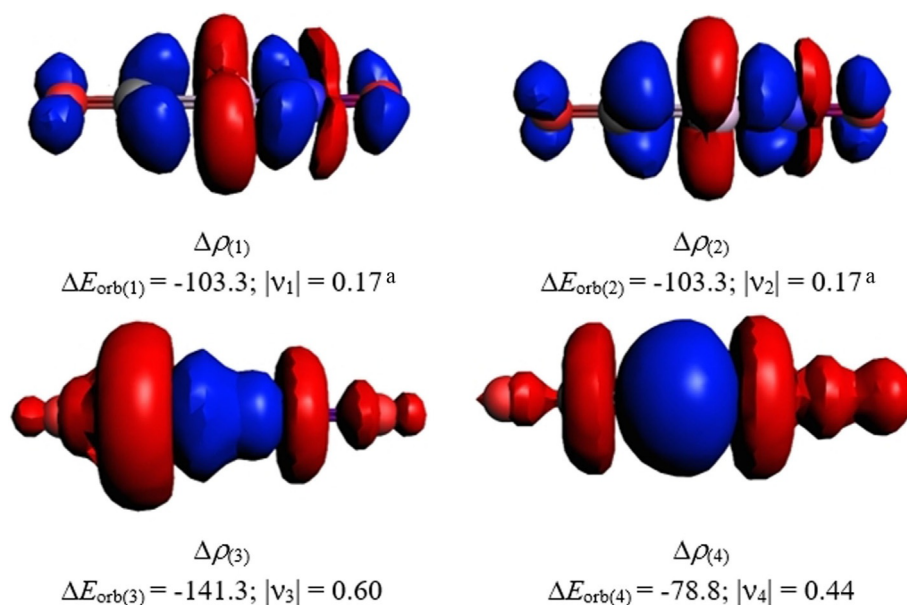


Figure 4. Shape of the deformation densities $\Delta\rho_{(1)-(4)}$ of the OCBNO molecule **A** associated with the orbital interactions $\Delta E_{\text{orb}(1)-(4)}$ at the M06-2X/TZ2P//CCSD(T)-Full/aug-cc-pVTZ level of theory (Table 2). Isosurface values are 0.001 au. The eigenvalues $|\nu_n|$ give the magnitude of the charge migration in electrons. The direction of the charge flow is red \rightarrow blue. ^a The net electron transfer in electron-sharing bonding.

5c-2e OCBNO π -bonds (ON = 2.00 for each orbital)Figure 5. Plot of the AdNDP orbitals of the π bonds in OCBNO (A).

atoms with carbon monoxide and nitric oxide in a solid neon matrix. This association reaction is predicted to be exothermic by $128.1 \text{ kcal mol}^{-1}$ at 0 K and requires negligible activation energy, as the OCBNO absorptions increase on annealing. The OCBNO molecule rearranges to the OBNCO isomer under UV excitation. This isomerization reaction is predicted to be exothermic by $111.9 \text{ kcal mol}^{-1}$ at the CCSD(T)-Full/aug-cc-pVTZ level of theory. The OCBNO \rightarrow OBNCO isomerization reaction on the singlet ground-state potential-energy surface is computed to proceed via an intermediate with a highly activated (1.601 \AA) side-on-bonded NO ligand (Figure S7 of the Supporting Information). The barrier from OCBNO to OBNCO is predicted to be $64.0 \text{ kcal mol}^{-1}$ at the CCSD(T)-Full/aug-cc-pVTZ//M06-2X-D3/aug-cc-pVTZ level of theory.

Conclusion

We have reported the synthesis of two isomers of BCNO_2 and their identification by matrix-isolation IR spectroscopy and quantum chemical calculations. The OCBNO complex, which is produced by the reaction of boron atoms with mixtures of carbon monoxide and nitric oxide in solid neon, rearranges to the more stable OBNCO isomer under UV excitation. Bonding analysis indicates that the OCBNO complex is best described by the bonding interactions between a triplet-state boron cation with an electron configuration of $(2s)^0(2p_\sigma)^0(2p_\pi)^2$ and the CO/NO $^-$ ligands in the triplet state forming two degenerate electron-sharing π bonds and two ligand-to-boron dative σ bonds.

Experimental Section

The 1064 nm fundamental output of a Nd:YAG laser (Continuum, Minilite II; 10 Hz repetition rate) with 5–15 mJ/pulse was used to ablate a rotating bulk boron target to produce boron atoms. The laser-evaporated boron atoms were codeposited with premixed carbon monoxide and nitric oxide reagent gases in excess neon onto a cryogenic CsI window, which was maintained at 4 K by means of a closed-cycle helium refrigerator. The CO/NO/Ne mixtures were prepared in a stainless steel vacuum line by using a standard manometric technique. Natural-abundance boron (19.8% ^{10}B , 80.2% ^{11}B) and ^{10}B -enriched (97%) targets were used in different experiments. The CO (Arkonic Gases & Chemical Inc., >99.99%), NO (Dalian DT, >99.9%), and isotopically labeled ^{13}CO , C^{18}O (ISOTECH, 99%), and ^{15}NO (Cambridge Isotope Laboratories Inc., 98%) were used without further purification. After 30 min of sample deposition at 4 K, IR absorption spectra in the mid-infrared

region ($4000\text{--}450 \text{ cm}^{-1}$) were recorded with a Bruker Vertex 80V spectrometer at 0.5 cm^{-1} resolution by using a liquid-nitrogen-cooled HgCdTe (MCT) detector. Bare-window background, recorded prior to sample deposition, was used as reference in processing the sample spectra. After the IR spectrum of the initial deposit had been recorded, the samples were warmed to the desired temperature, quickly recooled, and more spectra were taken. Photolysis was performed with a high-pressure mercury arc lamp.

The geometrical optimization and the evaluation of vibrational spectra of different isomers of BCNO_2 (A–O) were carried out at the CCSD(T)-Full/cc-pVTZ^[32] and B2PLYP/aug-cc-pVTZ levels of theory.^[33] To get better energetics, further reoptimizations followed by frequency calculations of the observed species, A and B were performed at the CCSD(T)-Full/aug-cc-pVTZ^[32] level of theory. All isomers presented here are minima on the potential-energy surface, as revealed by all-real frequencies. These calculations were performed with the Gaussian 16 program package.^[34] The natural bond orbital (NBO) analysis was done with the NBO 6.0 program.^[35] The AdNDP^[40] calculations were carried out with the program Multiwfn.^[41]

To shed light into the bonding situation in A, an energy decomposition analysis (EDA)^[36] together with the natural orbitals for chemical valence (NOCV)^[37] method was carried out by using the ADF 2018.105 program package.^[38] The EDA-NOCV calculations were carried out at the M06-2X/TZ2P^[39]//CCSD(T)-Full/aug-cc-pVTZ level of theory. For further information, see Supporting Information.

Acknowledgements

G.F. and L.Z. thank the financial support from Nanjing Tech University (Grant No. 39837132 and 39837123), National Natural Science Foundation of China (Grant No. 21703099, 21973044, 21688102), Natural Science Foundation of Jiangsu Province for Youth (Grant No: BK20170964), and SICAM Fellowship from Jiangsu National Synergetic Innovation Center for Advanced Materials. Open access funding enabled and organized by Projekt DEAL.

Conflict of interest

The authors declare no conflict of interest.

Keywords: ab initio calculations · bonding analysis · boron · IR spectroscopy · matrix isolation

[1] a) R. L. Melen, *Science* **2019**, *363*, 479–484; b) L. L. Zhao, S. Pan, N. Holzmann, P. Schwerdtfeger, G. Frenking, *Chem. Rev.* **2019**, *119*, 8781–8845;

- c) P. P. Power, *Chem. Rev.* **1999**, *99*, 3463–3503; d) H. J. Himmel, A. J. Downs, T. M. Greece, *Chem. Rev.* **2002**, *102*, 4191–4241.
- [2] a) P. Pyykkö, N. Runeberg, *J. Mol. Struct. Theochem* **1991**, *234*, 279–290; b) P. Pyykkö, *Phys. Chem. Chem. Phys.* **2012**, *14*, 14734–14742.
- [3] I. S. K. Kerkines, A. Papakondylis, A. Mavridis, *J. Phys. Chem. A* **2002**, *106*, 4435–4442.
- [4] S. Riedel, M. Straka, P. Pyykkö, *J. Mol. Struct. Theochem.* **2008**, *860*, 128–136.
- [5] D. S. Patel, P. V. Bharatam, *J. Phys. Chem. A* **2011**, *115*, 7645–7655.
- [6] M. A. Celik, R. Sure, S. Klein, R. Kinjo, G. Bertrand, G. Frenking, *Chem. Eur. J.* **2012**, *18*, 5676–5692.
- [7] O. Diels, B. Wolf, *Ber. Dtsch. Chem. Ges.* **1906**, *39*, 689–697.
- [8] a) P. Jensen, J. W. C. Johns, *J. Mol. Spectrosc.* **1986**, *118*, 248–266; b) J. Koput, *Chem. Phys. Lett.* **2000**, *320*, 237.
- [9] W. L. Burdick, *J. Am. Chem. Soc.* **1925**, *47*, 1485–1490.
- [10] a) B. V. Lotsch, J. Senker, W. Kockelmann, W. Schnick, *J. Solid State Chem.* **2003**, *176*, 180–191; b) B. Jagoda-Cwiklik, X.-B. Wang, H.-K. Woo, J. Yang, G.-J. Wang, M. F. Zhou, P. Jungwirth, L. S. Wang, *J. Phys. Chem. A* **2007**, *111*, 7719–7725; c) C. M. Nichols, Z. C. Wang, Z. B. Yang, W. C. Lineberger, V. M. Bierbaum, *J. Phys. Chem. A* **2016**, *120*, 992–999.
- [11] a) K. O. Christe, W. W. Wilson, J. A. Sheehy, J. A. Boatz, *Angew. Chem. Int. Ed.* **1999**, *38*, 2004–2009; *Angew. Chem.* **1999**, *111*, 2112–2118; b) A. Viji, W. W. Wilson, V. Vij, F. S. Tham, J. A. Sheehy, K. O. Christe, *J. Am. Chem. Soc.* **2001**, *123*, 6308–6313.
- [12] I. Bernhardt, T. Drews, K. Seppelt, *Angew. Chem. Int. Ed.* **1999**, *38*, 2232–2233; *Angew. Chem.* **1999**, *111*, 2370–2372.
- [13] Q. N. Zhang, W.-L. Li, C.-Q. Xu, M. H. Chen, M. F. Zhou, J. Li, D. M. Andradá, G. Frenking, *Angew. Chem. Int. Ed.* **2015**, *54*, 11078–11083; *Angew. Chem.* **2015**, *127*, 11230–11235.
- [14] a) W. H. Hocking, M. C. L. Gerry, *J. Mol. Spectrosc.* **1976**, *59*, 338–354; b) S. C. Ross, *J. Mol. Spectrosc.* **1988**, *132*, 48–79; c) C. L. Schmidt, D. Fischer, H. J. Himmel, R. Koeppel, H. Schnoekel, M. Jansen, *Z. Anorg. Allg. Chem.* **2009**, *635*, 1172–1178.
- [15] a) M. Feher, T. Pasinszki, T. Veszpremi, *Inorg. Chem.* **1995**, *34*, 945–951; b) J. O. Jensen, *J. Mol. Struct. Theochem.* **2005**, *715*, 1–5; c) M. K. Georgieva, I. G. Binev, *J. Mol. Struct.* **2005**, *752*, 14–19.
- [16] a) T. Brubacher, R. K. Bohn, W. Jager, M. C. L. Gerry, T. Pasinszki, N. P. C. Westwood, *J. Mol. Spectrosc.* **1997**, *181*, 316–322; b) J. Koput, *J. Phys. Chem. A* **2001**, *105*, 11347–11350; c) H. Lichau, S. C. Ross, M. Lock, S. Albert, B. P. Winnewisser, M. Winnewisser, F. C. De Lucia, *J. Phys. Chem. A* **2001**, *105*, 10080–10088; d) B. J. Guo, T. Pasinszki, N. P. C. Westwood, K. Q. Zhang, P. F. Bernath, *J. Chem. Phys.* **1996**, *105*, 4457–4460; e) T. Pasinszki, N. P. C. Westwood, *J. Phys. Chem.* **1996**, *100*, 16856–16863.
- [17] M. T. Nguyen, P. Ruelle, T.-K. Ha, *J. Mol. Struct.* **1983**, *104*, 353–364.
- [18] G. J. Wang, M. F. Zhou, *Int. Rev. Phys. Chem.* **2008**, *27*, 1–25.
- [19] M. F. Zhou, N. Tsumori, L. Andrews, Q. Xu, *J. Phys. Chem. A* **2003**, *107*, 2458–2463.
- [20] M. F. Zhou, Z. X. Wang, P. R. Schleyer, Q. Xu, *Chem. Phys. Chem.* **2003**, *4*, 763–766.
- [21] M. F. Zhou, N. Tsumori, Z. H. Li, K. N. Fan, L. Andrews, Q. Xu, *J. Am. Chem. Soc.* **2002**, *124*, 12936–12937.
- [22] a) P. Hassanzadeh, L. Andrews, *J. Phys. Chem.* **1992**, *96*, 9177–9182; b) L. Andrews, P. Hassanzadeh, T. R. Burkholder, *J. Chem. Phys.* **1993**, *98*, 922–931.
- [23] a) H. Mongeot, H. R. Atchekzai, M. Fouassier, M. T. Forel, *J. Mol. Struct.* **1980**, *62*, 35–46; b) H. Goubeau, H. Gräbner, *Chem. Ber.* **1960**, *93*, 1379–1387; c) M. Alae, E. G. Livingstone, N. P. C. Westwood, *J. Am. Chem. Soc.* **1993**, *115*, 2871–2876; d) G. H. Deng, S. Pan, X. L. Dong, G. J. Wang, L. L. Zhao, M. F. Zhou, G. Frenking, submitted.
- [24] a) T. R. Burkholder, L. Andrews, *J. Chem. Phys.* **1991**, *95*, 8697–8709; b) M. F. Zhou, N. Tsumori, Q. Xu, G. P. Kushto, L. Andrews, *J. Am. Chem. Soc.* **2003**, *125*, 11371–11378; c) Y. Gong, M. F. Zhou, *J. Phys. Chem. A* **2008**, *112*, 5670–5675.
- [25] P. Pyykkö, S. Riedel, M. Patzschke, *Chem. Eur. J.* **2005**, *11*, 3511–3520.
- [26] P. Pyykkö, M. Atsumi, *Chem. Eur. J.* **2009**, *15*, 12770–12779.
- [27] H. J. Zhai, Q. Chen, H. Bai, S. D. Li, L. S. Wang, *Acc. Chem. Res.* **2014**, *47*, 2435–2445.
- [28] G. Frenking, *Angew. Chem. Int. Ed.* **2014**, *53*, 6040; *Angew. Chem.* **2014**, *126*, 6152.
- [29] L. Zhao, M. Hermann, N. Holzmann, G. Frenking, *Coord. Chem. Rev.* **2017**, *344*, 163–204.
- [30] a) A. Michalak, M. Mitoraj, T. Ziegler, *J. Phys. Chem. A* **2008**, *112*, 1933; b) M. P. Mitoraj, A. Michalak, T. Ziegler, *J. Chem. Theory Comput.* **2009**, *5*, 962; c) L. Zhao, M. von Hopffgarten, D. M. Andradá, G. Frenking, *WIREs Comput. Mol. Sci.* **2018**, *8*, e1345.
- [31] a) N. Holzmann, M. Hermann, G. Frenking, *Chem. Sci.* **2015**, *6*, 4089–4094; b) D. M. Andradá, G. Frenking, *Angew. Chem. Int. Ed.* **2015**, *54*, 12319–12324; *Angew. Chem.* **2015**, *127*, 12494–12500; c) C. Mohapatra, S. Kundu, A. N. Paesch, R. Herbst-Irmer, D. Stalke, D. M. Andradá, G. Frenking, H. W. Roesky, *J. Am. Chem. Soc.* **2016**, *138*, 10429–10432; d) L. T. Scharf, M. Andradá, G. Frenking, V. H. Gessner, *Chem. Eur. J.* **2017**, *23*, 4422–4434; e) M. Hermann, G. Frenking, *Chem. Eur. J.* **2017**, *23*, 3347–3356; f) D. C. Georgiou, L. Zhao, D. J. D. Wilson, G. Frenking, J. L. Dutton, *Chem. Eur. J.* **2017**, *23*, 2926–2934; g) Z. Wu, J. Xu, L. Sokolenko, Y. L. Yagupolskii, R. Feng, Q. Liu, Y. Lu, L. Zhao, I. Fernández, G. Frenking, T. Trabelsi, J. S. Francisco, X. Zeng, *Chem. Eur. J.* **2017**, *23*, 16566–16573; h) D. M. Andradá, J. L. Casalz-Sainz, A. M. Pendas, G. Frenking, *Chem. Eur. J.* **2018**, *24*, 9083–9089; i) R. Saha, S. Pan, G. Merino, P. K. Chattaraj, *Angew. Chem. Int. Ed.* **2019**, *58*, 8372–8377; *Angew. Chem.* **2019**, *131*, 17848; j) Q. Wang, S. Pan, Y. Wu, G. Deng, G. Wang, L. Zhao, M. Zhou, G. Frenking, *Angew. Chem. Int. Ed.* **2019**, *58*, 17365–17374; *Angew. Chem.* **2019**, *131*, 17526–17535.
- [32] a) G. D. Purvis III, R. J. Bartlett, *J. Chem. Phys.* **1982**, *76*, 1910; b) J. A. Pople, M. Head-Gordon, K. Raghavachari, *J. Chem. Phys.* **1987**, *87*, 5968; c) T. H. Dunning, Jr., *J. Chem. Phys.* **1989**, *90*, 1007; d) R. A. Kendall, T. H. Dunning, Jr., R. J. Harrison, *J. Chem. Phys.* **1992**, *96*, 6796; e) D. E. Woon, T. H. Dunning, Jr., *J. Chem. Phys.* **1993**, *98*, 1358; f) K. A. Peterson, D. E. Woon, T. H. Dunning, Jr., *J. Chem. Phys.* **1994**, *100*, 7410.
- [33] S. Grimme, *J. Chem. Phys.* **2006**, *124*, 034108.
- [34] Gaussian 16, Revision A.03, M. J. Frisch, G. W. Trucks, H. B. Schlegel, G. E. Scuseria, M. A. Robb, J. R. Cheeseman, G. Scalmani, V. Barone, G. A. Petersson, H. Nakatsuji, X. Li, M. Caricato, A. V. Marenich, J. Bloino, B. G. Janesko, R. Gomperts, B. Mennucci, H. P. Hratchian, J. V. Ortiz, A. F. Izmaylov, J. L. Sonnenberg, D. Williams-Young, F. Ding, F. Lipparini, F. Egidi, J. Goings, B. Peng, A. Petrone, T. Henderson, D. Ranasinghe, V. G. Zakrzewski, J. Gao, N. Rega, G. Zheng, W. Liang, M. Hada, M. Ehara, K. Toyota, R. Fukuda, J. Hasegawa, M. Ishida, T. Nakajima, Y. Honda, O. Kitao, H. Nakai, T. Vreven, K. Throssell, J. A. Montgomery, Jr., J. E. Peralta, F. Ogliaro, M. J. Bearpark, J. J. Heyd, E. N. Brothers, K. N. Kudin, V. N. Staroverov, T. A. Keith, R. Kobayashi, J. Normand, K. Raghavachari, A. P. Rendell, J. C. Burant, S. S. Iyengar, J. Tomasi, M. Cossi, J. M. Millam, M. Klene, C. Adamo, R. Cammi, J. W. Ochterski, R. L. Martin, K. Morokuma, O. Farkas, J. B. Foresman, D. J. Fox, Gaussian, Inc., Wallingford CT, **2016**.
- [35] E. D. Glendenning, C. R. Landis, C. F. Weinhold, *J. Comput. Chem.* **2013**, *34*, 1429.
- [36] T. Ziegler, A. Rauk, *Theor. Chim. Acta* **1977**, *46*, 1–10.
- [37] a) M. Mitoraj, A. Michalak, *Organometallics* **2007**, *26*, 6576; b) M. Mitoraj, A. Michalak, *J. Mol. Model.* **2008**, *14*, 681.
- [38] a) ADF2018, SCM, Theoretical Chemistry, Vrije Universiteit, Amsterdam, The Netherlands, <http://www.scm.com>; b) G. te Velde, F. M. Bickelhaupt, E. J. Baerends, C. F. Guerra, S. J. A. Van Gisbergen, J. G. Snijders, T. Ziegler, *J. Comput. Chem.* **2001**, *22*, 931.
- [39] E. van Lenthe, E. J. Baerends, *J. Comput. Chem.* **2003**, *24*, 1142.
- [40] D. Y. Zubarev, A. I. Boldyrev, *Phys. Chem. Chem. Phys.* **2008**, *10*, 5207.
- [41] T. Lu, F. Chen, *Chem. Eur. J.* **2011**, *33*, 580.

Manuscript received: August 22, 2020

Accepted manuscript online: October 26, 2020

Version of record online: December 3, 2020